

Synthesis and Biological Studies of a New Series of 5-Heteroarylcarbamoylaminopyrazolo[4,3-*e*]1,2,4-triazolo[1,5-*c*]pyrimidines as Human A₃ Adenosine Receptor Antagonists. Influence of the Heteroaryl Substituent on Binding Affinity and Molecular Modeling Investigations

Giorgia Pastorin,[†] Tatiana Da Ros,[†] Chiara Bolcato,[†] Christian Montopoli,[‡] Stefano Moro,^{*,‡} Barbara Cacciari,[§] Pier Giovanni Baraldi,[§] Katia Varani,[⊥] Pier Andrea Borea,[⊥] and Giampiero Spalluto^{*,†}

Dipartimento di Scienze Farmaceutiche, Università degli Studi di Trieste, Piazzale Europa 1, I-34127 Trieste, Italy, Dipartimento di Scienze Farmaceutiche, Università degli Studi di Ferrara, Via Fossato di Mortara 17-19, I-44100 Ferrara, Italy, Molecular Modeling Section, Dipartimento di Scienze Farmaceutiche, Università di Padova, via Marzolo 5, I-35131 Padova, Italy, and Dipartimento di Medicina Clinica e Sperimentale - Sezione di Farmacologia, Università degli Studi di Ferrara, Via Fossato di Mortara 17-19, I-44100 Ferrara, Italy

Received November 15, 2005

Some pyrazolotriazolopyrimidines bearing different heteroarylcarbamoylamino moieties at the N5-position are described. We previously reported the synthesis of a water soluble compound with high potency and selectivity versus the human A₃ adenosine receptor as antagonist, and herein we present an enlarged series of compounds related to the previously mentioned one. These compounds showed A₃ adenosine receptor affinity in the nanomolar range and different levels of selectivity evaluated in radioligand binding assays at human A₁, A_{2A}, A_{2B}, and A₃ adenosine receptors. In particular, the effect of the heteroaryl substituents at the N5 position has been analyzed. This study allows us to recognize that the presence of a pyridinium moiety in this position not only increases water solubility but also improves or retains potency and selectivity at the human A₃ adenosine receptors. In contrast, replacement of pyridine with different heterocycles produces loss of affinity and selectivity at the human A₃ adenosine receptors. A molecular modeling study has been carried out with the aim to explain these various binding profiles.

Introduction

Interaction of adenosine with its receptors, classified as A₁, A_{2A}, A_{2B}, and A₃, could modulate several physiological functions. These receptor subtypes belong to the family of the G protein coupled receptors and exert their physiological role by activation or inhibition of different second messenger systems.^{1,2}

In recent years, intense efforts by medicinal chemists have led to the discovery of several potent and selective adenosine receptor agonists and antagonists, which permitted the pharmacological characterization of this family of G-protein coupled receptors. In particular A₁, A_{2A}, and A₃ subtypes have been well characterized through the use of potent and selective ligands.^{1,3}

The A₃ adenosine receptor subtype has been cloned from different species (e.g. rat, human, dog, sheep),^{4–9} and it is found to modulate two second messenger systems: inhibition of adenylyl cyclase³ and stimulation of phospholipase C¹⁰ and D.¹¹ The potential therapeutic applications of activating or antagonizing this receptor subtype have been investigated in recent years. In particular, antagonists for the A₃ receptor promise to be useful for the treatment of inflammation¹² and in the regulation of the cell growth.^{13,14}

In this field, many different classes of compounds have been proposed, with both good affinity (nM range) and selectivity.^{15–17} In particular our group proposed a series of pyrazolo-triazolo-pyrimidines^{18–22} which proved to be the most potent and

selective human A₃ adenosine receptors ever reported (e.g. compounds **1** and **2**).²⁰ (Chart 1) Unfortunately, a major problem of these compounds is the typical low water solubility, which has limited their use as pharmacological and diagnostic tools. This aspect has been avoided with the synthesis, previously reported in a preliminary form, of derivative **3** (5-[[[4-pyridyl]-amino]carbonyl]amino-8-methyl-2-(2-furyl)-pyrazolo[4,3-*e*]-1,2,4-triazolo[1,5-*c*]pyrimidine hydrochloride);²² this derivative was highly water soluble (15 mM) and also displayed a significantly increased potency and selectivity at the A₃ adenosine receptor with respect to the reference compounds **1** and **2** (Chart 1).

This exceptional potency has preliminarily been rationalized by a molecular modeling investigation.²² Our pilot docking studies have highlighted a strong electrostatic interaction among the pyridinium moiety of **3** and two carbonyl backbone moieties of the TM region of human A₃ adenosine receptor.²² These electrostatic interactions might be responsible for the increase of the affinity in the protonated form, i.e., the hydrochloride derivative **3**.

To strengthen our preliminary modeling studies, we synthesized an enlarged series of N⁸-methyl pyrazolo-triazolo-pyrimidines bearing different heteroarylcarbamoyl moieties (**4–20**) at the 5-position. In particular: (i) the position of the nitrogen on pyridine nucleus was modified, (ii) the basicity of pyridine nitrogen was deleted by formation of N-oxide or N-methyl derivatives, (iii) the pyridine moiety was replaced with different heteroaryl groups (Chart 2).

Chemistry. The desired compounds (**4**, **5**, **7**, **15–20**) were prepared by reaction of the appropriate acyl azides **21–29** (2 equiv), obtained from commercially available acid and diphenylphosphoryl azide (DPPA),²³ and the well-known methyl derivative **30**¹⁹ in dry dioxane at reflux (18 h). Under these

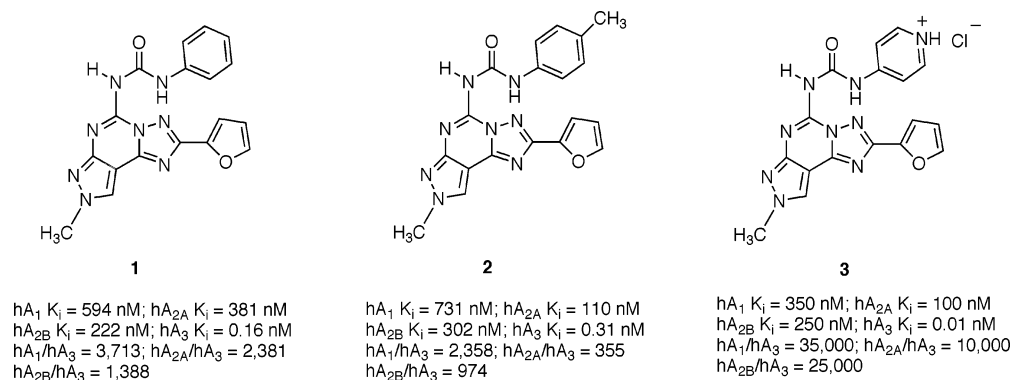
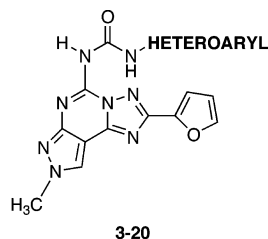
* To whom correspondence should be addressed. (G.P.) Phone: +39 040 5583726, fax: +39 040 52572, e-mail: spalluto@univ.trieste.it.

[†] Università degli Studi di Trieste.

[§] Dipartimento di Scienze Farmaceutiche, Università degli Studi di Ferrara.

[‡] Università di Padova.

[⊥] Dipartimento di Medicina Clinica e Sperimentale - Sezione di Farmacologia, Università degli Studi di Ferrara.

Chart 1. Structures and Binding Affinities at the Four Adenosine Receptor Subtypes of Reference Compounds**Chart 2.** General Structures of Designed and Synthesized Compounds

**ARYL = 2-,3-,4-pyridyl, 2-,3-,4-pyridyl hydrochlorides;
 2-,3-,4-N-methyl pyridinium salts, 2-,3-,4-yrindinium N-oxide
 2-, 3-furyl, 2-, 3-thienyl, 2-benzofuranyl, 2-quinolinyl**

condition, the acyl azide led to appropriate isocyanate by Curtius rearrangement,²⁴ which reacted with the amino function to give the final compounds (Scheme 1).

The pyridine derivatives as hydrochlorides (**3**, **6**, **8**) were prepared by treating the free base (**4**, **5**, **7**) for 30 min at 0 °C with methanol saturated with HCl gas. The corresponding *N*-methylpyridinium salt (**9–11**) and the *N*-oxide derivatives (**12–14**) were obtained by treating the pyridine analogues (**4**, **5**, **7**) with methyl iodide or 3-chloroperbenzoic acid, respectively, under standard conditions (Scheme 2).

The regioselective preparation of N8 methyl derivative **30** was novel. Up to now we reported the synthesis of N⁸-substituted pyrazolo-triazolo-pyrimidines by standard procedure, described by Gatta and co-workers,²⁵ starting from the appropriate alkylated 5-amino-4-cyanopyrazole.¹⁹ The alkylation performed under typical conditions (NaH, in dry DMF) using a small alkylating agent led to a 1:1 mixture of two regioisomers with a consequent reduction of final yield. To overcome this problem, we regioselectively prepared *N*²-methyl-4-cyano-5-aminopyrazole **31** following a well-known procedure.^{26,27}

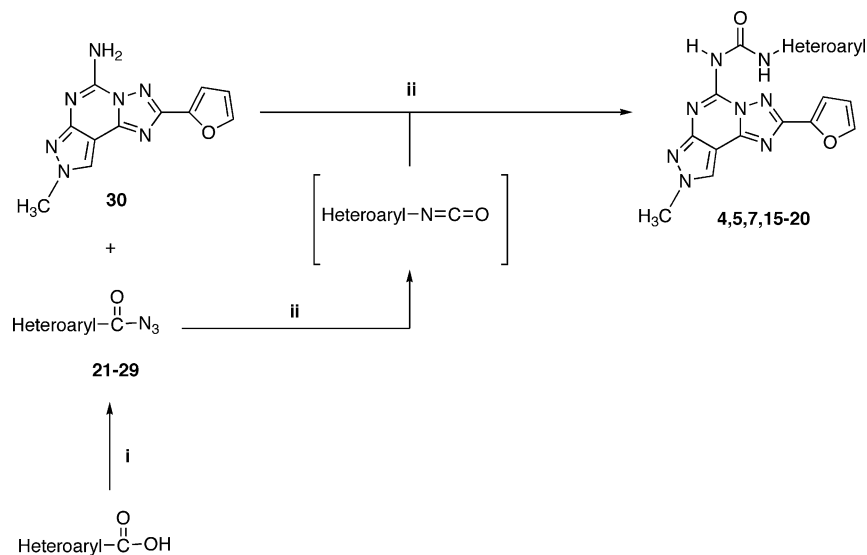
Results and Discussion

In Table 1 the receptor binding affinities of the synthesized compounds (**3–20**) are reported. They were determined at the human A₁, A_{2A}, and A₃ receptors expressed in CHO (A₁, A_{2A}, A₃) cells; [³H]-1,3-dipropyl-8-cyclopentylxanthine ([³H]DPCPX) (A₁),^{28,29} [³H]-4-[2-[[7-amino-2-(2-furyl)[1,2,4]-triazolo[2,3-*a*]-[1,3,5]triazin-5-yl]amino]ethyl]phenol ([³H]-ZM241385) (A_{2A}),³⁰ and [³H]-5-(4-methoxyphenylcarbamoyl)amino-8-propyl-2-(2-furyl)-pyrazolo[4,3-*e*]-1,2,4-triazolo[1,5-*c*]pyrimidine ([³H]-MRE3008-F20) (A₃)²⁹ have been used as radioligands in binding assays.

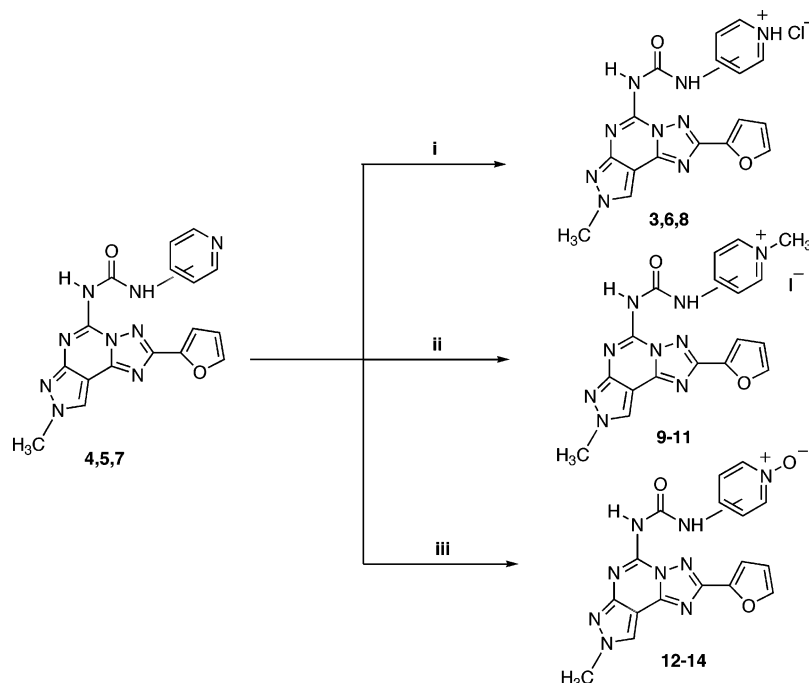
To evaluate the potency at human A_{2B} receptors, due to the lack of a suitable radioligand, the activity of antagonists was determined in a functional assay based on the antagonism of NECA (100 nM)-induced stimulation of cyclic AMP levels. All

the synthesized compounds showed affinity in the low nanomolar range for the human A₃ adenosine receptors with different degrees of selectivity versus the other receptor subtypes. Pyridine derivatives **3–8** showed the best profile in terms of both affinity and selectivity at the hA₃ adenosine receptors, and no significant differences emerged comparing the free bases (**4**, **5**, **7**) and the hydrochloride forms (**3**, **6**, **8**); nevertheless, the salts present an exceptional water solubility (15 mM), which renders these derivatives as ideal candidates for pharmacological studies. On the other hand, it should be noted that the nitrogen position on the pyridine nucleus significantly influences affinity at the human A₃ adenosine receptors with a consequent reduction of selectivity versus the other receptor subtypes. In fact the best affinity at the A₃ receptors was obtained by using the 4-pyridyl moiety (0.014–0.04 nM), while a significant reduction of affinity (10–30-fold) was observed when nitrogen was at the 3- or 2-position. These results strongly suggested that the electrostatic interactions hypothesized for derivative **3**²² were not possible with the other isomers (**5–8**), and these compounds showed an affinity versus the human A₃ adenosine receptors very similar to reference compound **1** (e.g. compound **5**: *K*_i hA₃ 0.44 nM vs compound **1**: *K*_i hA₃ 0.16 nM).

A completely different biological profile was observed when pyridine nitrogen was alkylated or oxidized. In the *N*-methylpyridinium series (**9–11**) a significant reduction of binding affinity at the human A₃ adenosine receptors (ranging from 1.3 to 28 nM) with respect to the pyridine analogues **3–8** was obtained (100–2000-fold). Moreover the position of the *N*-methylpyridinium moiety demonstrated a strong effect on binding affinity, which seems to contradict the experimental observations made for the pyridine analogues **3–8**. In fact derivative **9** was the least potent of this series (*K*_i hA₃ 28 nM) while compound **11** showed a recovered potency at the hA₃ adenosine receptors (*K*_i hA₃ 1.3 nM). These results suggested that the presence of the methylpyridinium moiety had a negative effect on binding affinity at the hA₃ adenosine receptors. Comparing binding affinities of reference compound **2** (Chart 1) to its bioisostere **9**, a reduction of almost 100 fold in terms of affinity at the hA₃ adenosine receptors was observed (compound **2**: *K*_i hA₃ 0.31 nM vs compound **9**: *K*_i hA₃ 28 nM). As we clarify later in the modeling discussion, we found a reasonable interpretation of these data based on the ligand–receptor complementarity analysis. Interestingly, it should be also noted that an *N*-methylpyridinium salt at the 2- or 3-positions induces good potency on 100 nM NECA-stimulated cAMP accumulation in CHO cells expressing hA_{2B} receptors (244–280 nM), while compounds **3–8** and the 4-*N*-methylpyridinium derivative **9** did not bind this receptor subtype at concentrations up to 1 μM.

Scheme 1. Synthesis of **4**, **5**, **7**, **15–20**^a

^a Reagents and conditions: i: DMF, DPPA, Et₃N, ii: dioxane reflux, 18 h.

Scheme 2. Synthesis of **3**, **6**, **8–14**^a

^a Reagents and conditions: i: MeOH, HCl gas, 0 °C, 30 min; ii: MeCN, MeI, 40 °C, 5 h; iii: THF, mCPBA, rt, 12 h.

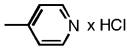
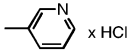
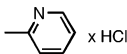
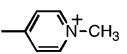
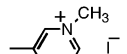
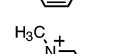
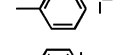
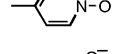
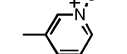
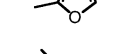
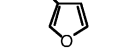
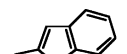
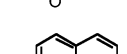
All these observations are strongly supported by the analysis of binding data for the pyridinium *N*-oxide series (**12–14**), which are exactly the same. In fact derivative **12** showed an affinity for the hA₃ adenosine receptors comparable with the 4-*N*-methylpyridinium derivative **9** (compound **12**: *K*_i hA₃ 21 nM vs compound **9**: *K*_i hA₃ 28 nM). Similarly, as mentioned above for derivatives **9–11**, the 2- and 3-pyridinium *N*-oxide derivatives (**13**, **14**) possess a better affinity for the hA₃ adenosine receptor subtype with respect to the 4-pyridinium derivative (**13**: *K*_i hA₃ 10 nM vs **10**: *K*_i hA₃ 5.3 nM; **14**: *K*_i hA₃ 3.5 nM vs **11**: *K*_i hA₃ 1.3 nM). Also in this series, derivatives **13** and **14** proved to be quite potent versus the hA_{2B} adenosine receptor subtype.

A quite different biological profile was found when the pyridine moiety was replaced with other heterocycles. Substitution with a furan ring, linked at the 2- (**15**) or 3-position (**16**),

induces a significant decrease of affinity of more than 100 fold (e.g. compound **3**: *K*_i hA₃ 0.046 nM vs compound **15**: *K*_i hA₃ 16 nM). Most surprisingly, the replacement with thiophene (**19**, **20**)³¹ produced a significant reduction of affinity not only with respect to the pyridine derivative **3**, but also with respect to reference compound **2** (e.g. compound **2**: *K*_i hA₃ 0.16 nM vs compound **20**: *K*_i hA₃ 3.5 nM).

If more complex heteroaryl systems such as benzofuran (**17**) or quinoline (**18**) were introduced at the 5-position, a significant decrease of affinity at the hA₃ adenosine receptors was generally observed, but while the introduction of a benzofuryl moiety (**17**) retains a quite good affinity at the hA₃ receptors (*K*_i hA₃ 12 nM) and also at the A_{2A} (*K*_i hA_{2A} 60 nM) and A_{2B} (IC₅₀ hA_{2B} 250 nM) subtypes, the quinoline nucleus (**18**) induces a significant decrease of affinity at all four adenosine receptor subtypes.

Table 1. Structures and Binding Affinity at hA₁, hA_{2A}, hA₃ and Potency at hA_{2B} Adenosine Receptors of Synthesized Compounds (3–20)

| Compd. | Aryl | hA ₁ (K _i , nM) ^a | hA _{2A} (K _i , nM) ^b | hA _{2B} IC ₅₀ (nM) ^c | hA ₃ (K _i , nM) ^d | hA ₁ /hA ₃ | hA _{2A} /hA ₃ |
|--------|---|--|---|---|--|----------------------------------|-----------------------------------|
| 4 |  | 260 ± 30 ^e | 65 ± 10 ^e | > 1000 (20%) | 0.046 ± 0.010 ^e | 5650 | 1413 |
| 3 |  | 355 ± 25 ^e | 110 ± 15 ^e | > 1000 (12%) | 0.014 ± 0.006 ^e | 25357 | 7857 |
| 5 |  | 230 ± 20 | 125 ± 12 | > 1000 (24%) | 0.44 ± 0.20 | 522 | 284 |
| 6 |  | 245 ± 25 | 155 ± 25 | > 1000 (18%) | 0.55 ± 0.10 | 445 | 281 |
| 7 |  | 210 ± 24 | 140 ± 35 | > 1000 (16%) | 0.35 ± 0.10 | 600 | 400 |
| 8 |  | 265 ± 28 | 180 ± 18 | > 1000 (20%) | 0.50 ± 0.15 | 530 | 360 |
| 9 |  | > 1000 (20%) | 282 ± 35 | > 1000 (6%) | 28 ± 3 | > 36 | 10 |
| 10 |  | 330 ± 35 | 42 ± 6 | 244 ± 28 | 5.3 ± 0.8 | 62 | 8 |
| 11 |  | 400 ± 43 | 64 ± 8 | 280 ± 32 | 1.3 ± 0.2 | 307 | 49 |
| 12 |  | > 1000 (35%) | 153 ± 18 | > 1000 (12%) | 21 ± 3 | > 47 | 7.3 |
| 13 |  | 550 ± 62 | 75 ± 9 | 260 ± 22 | 10 ± 2 | 55 | 7.5 |
| 14 |  | 800 ± 84 | 110 ± 15 | 320 ± 35 | 3.5 ± 0.4 | 228 | 31 |
| 15 |  | > 1000 (25%) | 350 ± 38 | > 1000 (8%) | 16 ± 3 | > 62.5 | 22 |
| 16 |  | > 1000 (20%) | 400 ± 45 | > 1000 (4%) | 11 ± 2 | > 90 | 36 |
| 17 |  | > 1000 (22%) | 60 ± 8 | 250 ± 30 | 12 ± 2 | > 83 | 5 |
| 18 |  | > 1000 (12%) | 810 ± 72 | > 1000 (17%) | 110 ± 35 | > 9 | 7.3 |
| 19 |  | > 1000 (10%) | 920 ± 83 | > 1000 (20%) | 10 ± 1 | > 100 | 92 |
| 20 |  | > 1000 (24%) | 410 ± 35 | > 1000 (31%) | 3.5 ± 0.4 | > 286 | 117 |

^a Displacement of specific [³H]-DPCPX binding at human A₁ receptors expressed in CHO cells (*n* = 3–6). ^b Displacement of specific [³H]-ZM241385 binding at human A_{2A} receptors expressed in HEK-293 cells. ^c IC₅₀ values of the inhibition of the tested compounds on 100 nM NECA-stimulated cAMP accumulation in CHO cells expressing hA_{2B} receptors. ^d Displacement of specific [³H]MRE3008-F20 binding at human A₃ receptors expressed in HEK-293 cells. Data are expressed as means, with ± SEM. Data in parentheses are expressed as percentage of inhibition of specific binding at a concentration of 1 μM of the tested compounds. ^e Data taken from ref 22.

A new series of docking simulations have been carried out to better rationalize the experimental binding affinities of all newly synthesized *N*⁸-methylpyrazolo-triazolo-pyrimidines bearing different heteroarylcarbomoyl moieties (4–20) at the 5-position.

Following our recently reported modeling approaches, we used an improved model of the human A₃ receptor, obtained by a rhodopsin-based homology modeling approach, to recognize the hypothetical binding motif of these new water soluble

human A₃ antagonists.^{16,32,33} Considering docking simulations, all new pyrazolo-triazolo-pyrimidine derivatives share the common binding motif inside the TM region of human A₃ receptor, as previously described.^{16,32,33} Before starting the molecular modeling description of this new series of pyrazolo-triazolo-pyrimidine derivatives, it is very interesting to remember that derivative 3 undergoes to the acid–base equilibrium, forming both protonated and unprotonated forms as a function of the environment pH value. Of course, under buffer conditions

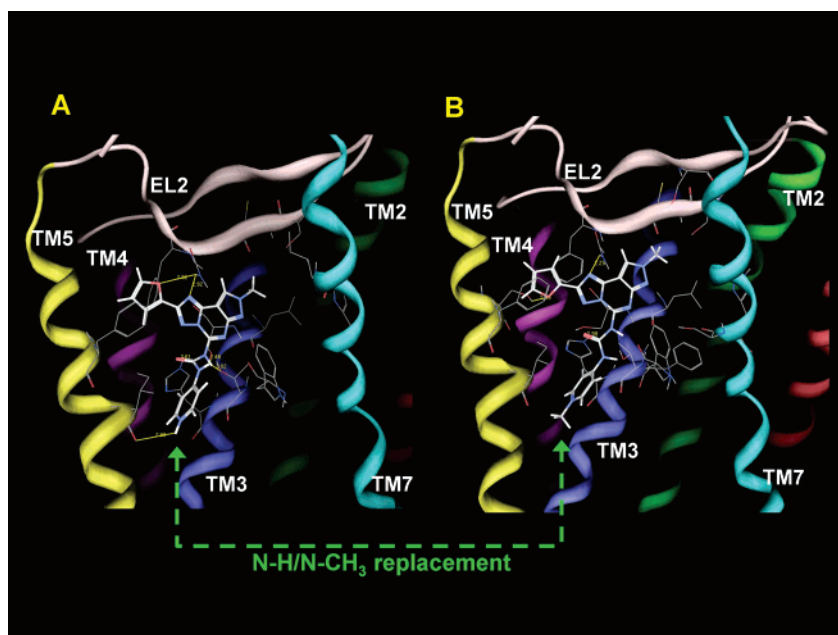


Figure 1. The general topology of the human A_3 receptor model. Reference compounds **3** (on the left) and **9** (on the right) are docked inside the transmembrane recognition site (see Experimental Section for details) viewed from the membrane side facing TM helices 5 and 6. To clarify the TM cavity viewing, TM6 has been voluntarily omitted. Side chains of some amino acids important for ligand recognition are highlighted.

both free base and hydrochloride give rise to the same equilibrium. On the contrary, the experimental data seem to indicate that the hydrochloride derivative presents a higher affinity compared with the free base.¹⁶ We have already speculated that the kinetic of the solubilization process might play a critical role in determining the final concentration of both compounds in solution. In this sense, hydrochloride solubilizes faster than the corresponding free base and, consequently, can guarantee a higher concentration of antagonist in solution. Moreover, we have also found that the best docking energy for the free base is around 20 kcal/mol less stabilizing compared to the corresponding protonated form of derivative **3**. We have explained this result as a sort of receptor-driven selection of the protonated versus the unprotonated form of the antagonist. Indeed, other positively charged antagonists have been already reported to be nicely accommodated into human A_3 binding region such as the water-soluble 3,5-diacyl-1,2,4-trialkylpyridinium salts already reported by K. A. Jacobson et al. (*J. Med. Chem.* **1999**, *42*, 4232). As we describe in detail later, from a molecular point of view, we have found that the TM5 region closed to Ile186 could mediate this stabilizing interaction.

As shown in Figure 1, we identified the hypothetical binding site of the pyrazolo-triazolo-pyrimidine moiety surrounded by TMs 3, 5, 6, and 7 with furan ring and the N^8 -substituents pointing toward the EL2, and the carbamoyl moiety in the 5-position oriented toward the intracellular environment. The furan ring is positioned between TM5 and TM3 whereas the N^8 -substituents are surrounded by TM2 and TM7. Interestingly, these pharmacophore feature models are nicely coherent with our recently proposed receptor-based pharmacophore model. Analyzing in detail our model, all pyrazolo-triazolo-pyrimidine derivatives present the carbamoyl moiety in the 5-position surrounded by two polar amino acids: His95 (TM3) and Ser247 (TM6). This region seems to be very critical for the recognition of the antagonist structures. In fact, a major structural difference between the hypothetical binding sites in these receptor subtypes is that the A_3 receptor does not contain the histidine residue in TM6 common to all A_1 (His251 in hA₁) and A_2 (His250 in hA_{2A}) receptors. This histidine has been shown to participate

in both agonist and antagonist binding to A_{2A} receptors. In the A_3 receptor this histidine in TM6 is replaced by a serine residue (Ser247 in hA₃).³⁴ The stabilizing interactions among the carbamoyl moiety and these polar amino acids orient the carbamoyl phenyl ring in the middle of the TM bundle. In particular, the N–H of His95 (TM3) and the oxygen atom of the carbamoyl group are separated by 2.6 Å and appropriately oriented to form an H-bonding interaction. The side chain of Ser247 (TM6) is within hydrogen-bonding distance of NH of the carbamoyl group at 2.9 Å. According to the recently published mutagenesis results, His95 is crucial for ligand recognition, whereas Ser247 slightly affects the binding of both agonists and antagonists.³⁴ The receptor region around the aryl or heteroaryl ring of the carbamoyl moiety is mostly hydrophobic and characterized by three nonpolar amino acids: Ile98 (TM3), Ile186 (TM5), Leu244 (TM6). However, a very strong charge-dipole interaction between the carbonyl backbone moiety of Ile186 (TM5) and the 4-pyridinium system of **3** seems to strongly influence the binding affinity versus the human A_3 receptor. The strength of this important charge-dipole interaction is greatly reduced in intensity for both 3-pyridinium (**6**) and 2-pyridinium (**8**) analogues as a consequence of the increased distance between the positive pyridinium charge of derivatives **3**, **6**, **8** and the carbonyl moiety of Ile186 (TM5), as shown in Figures 2–4. The evaluation of the ligand binding pocket of this specific region of the A_3 receptor reveals that a very limited empty space is present between TM5 and TM6, and consequently a severe steric control seems to take place around the 4-position of the aryl ring. As already demonstrated, substituents at the 4-position of the N^5 -phenyl ring of pyrazolo-triazolo-pyrimidine scaffold induced a decrease of affinity at the human A_3 adenosine receptors of about 2–5-fold with respect to the nonsubstituted derivatives.^{20,22} Using this argument, we can explain the drop of the activities of both *p*-*N*-methyl (**9**) and *p*-*N*-oxide (**12**) derivatives compared with the analogue **3**. Moreover, also the nature of electrostatic interactions among the carbonyl backbone moiety of Ile186 (TM5) and the positively charged *N*-methyl (**9**) or the zwitterionic *N*-oxide (**12**) groups are less effective than the positively charged 4-pyri-

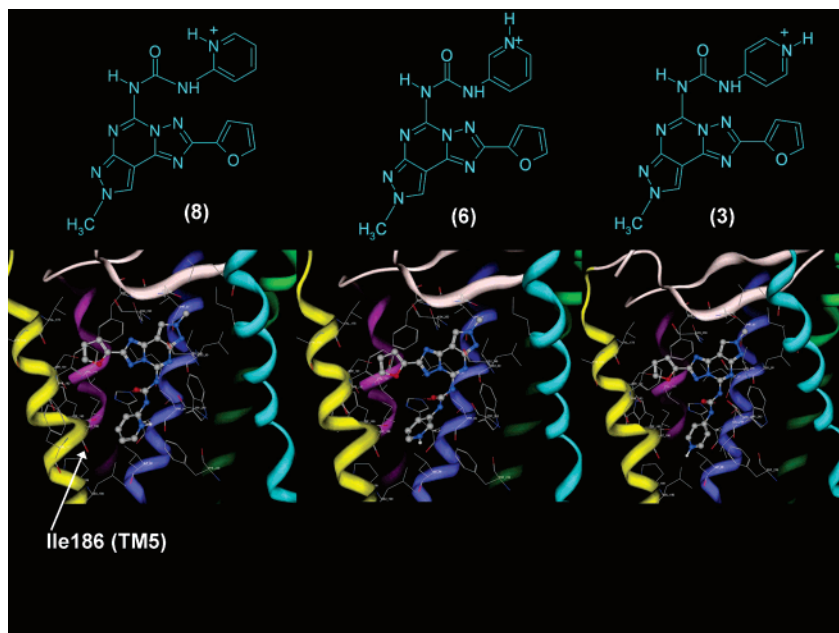


Figure 2. Molecular docking of ortho (**8**), meta (**6**) and para (**3**) pyridinium compounds. Side chains of some amino acids important for ligand recognition are highlighted.

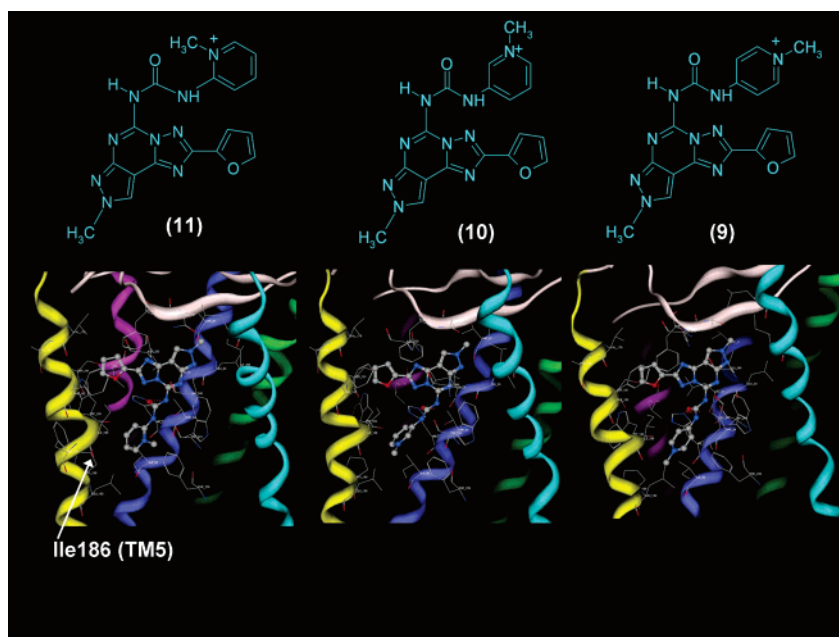


Figure 3. Molecular docking of ortho (**11**), meta (**10**) and para (**9**) methylpyridinium compounds. Side chains of some amino acids important for ligand recognition are highlighted.

dinium system of **3**. In fact from a chemical point of view, the carbonyl backbone moiety of Ile186 (TM5) interacts differently with the positively charged N–H of derivative **3** in which a hydrogen-mediated interaction is still possible with respect to the positively charged N–Me of derivative **9** that cannot establish a hydrogen-mediated interaction with the carbonyl backbone moiety of Ile186, and finally, with the formally neutral N⁺–O[–] moiety of derivative **12**. Accordingly, bulkier but planar substituents, such as benzofuran (**17**) or quinoline (**18**), also slightly reduce the receptor complementarity. Moreover, smaller heteroaromatic substituents such as methylthiophene (**19** and **20**) can be also accommodated into the recognition pocket, partially loosening the receptor shape complementarity (data not shown). However, it is useful to note that all the above-mentioned derivatives (**15**–**20**) are still active

at a low nanomolar range as human A₃ antagonists. Following our previously published results, substituents at the ortho position of the N⁵-phenyl ring of the pyrazolo-triazolo-pyrimidine scaffold seem to occupy an empty region of the binding receptor cavity.²⁰

As already described, in the chlorine-substituted series the change of the position (2- or 4-phenyl) does not seem to influence affinity at the human A₁, human A_{2A}, and human A_{2B} receptors compared with the 3-chloro-substituted compounds, maintaining it in the high nanomolar range (100–500 nM), while significant differences appeared in binding affinity to the human A₃ adenosine receptors.²⁰ Also with these newly synthesized *N*-methyl and *N*-oxide derivatives, we observed a similar chemical behavior. Indeed, both *o*-*N*-methyl (**11**) and *N*-oxide (**14**) derivatives are more active than the corresponding

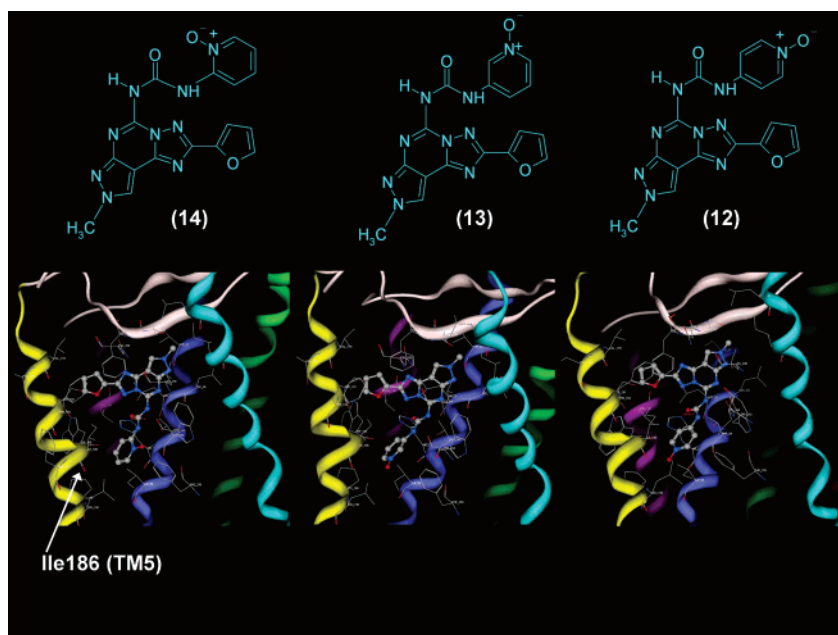


Figure 4. Molecular docking of ortho (**14**), meta (**13**) and para (**12**) NO compounds. Side chains of some amino acids important for ligand recognition are highlighted.

p-*N*-methyl (**9**) and *N*-oxide (**12**) isomers (see Table 1 and Figures 2–4).

Finally, a similar steric control takes place when substituents larger than hydrogen are also present at the 3-position of the aryl or heteroaryl ring. In this case, a steric repulsion among substituents, at the 4-position, and amino acid side chains of TM6 and TM7 could significantly reduce the affinity at the human A₃ receptor. Consistently, both *m*-*N*-methyl (**10**) and *N*-oxide (**13**) derivatives are less active than the corresponding *o*-*N*-methyl (**11**) and *N*-oxide (**14**) isomers (see Table 1 and Figures 2–4).

Conclusions

The present study provides important information concerning the structural requirements necessary for the recognition of the human A₃ adenosine receptor. In particular the effect of a heteroaryl carbamoyl moiety at the N⁵ position has been strongly investigated. It has been confirmed that a pyridinium moiety increases water solubility and increases or retains affinity and selectivity at the human A₃ adenosine receptor subtype. In particular the position of the nitrogen and its nature significantly influence both affinity and selectivity. In contrast, when the pyridinium moiety was replaced with other heterocycles, such as furan or thiophene, a significant reduction of both affinity and selectivity vs the hA₃ adenosine receptors was observed. All these experimental observations have been studied with molecular modeling simulation, permitting validation of the recently proposed receptor-based pharmacophore model.^{16,32}

Experimental Section

Chemistry. General. Reactions were routinely monitored by thin-layer chromatography (TLC) on silica gel (precoated F₂₅₄ Merck plates). Infrared spectra (IR) were measured on a Jasco FT-IT instrument. ¹H NMR were determined in CDCl₃ or DMSO-*d*₆ solutions with a Varian Gemini 200 spectrometer, peaks positions are given in parts per million (δ) downfield from tetramethylsilane as internal standard, and *J* values are given in Hz. Light petroleum ether refers to the fractions boiling at 40–60 °C. Melting points were determined on a Buchi-Tottoli instrument and are uncorrected. Electrospray mass spectra were recorded on a Perkin-Elmer PE SCIEX API 1 spectrometer, and compounds were dissolved in

methanol. Flash chromatography was performed using Merck 60–200 mesh silica gel. Elemental analyses were performed by the microanalytical laboratory of Dipartimento di Chimica, University of Trieste, and were within ±0.4% of the theoretical values for C, H, and N.

General Procedures for the Preparation of 5-Heteroarylcarbamoylamino-pyrazolo[4,3-*e*]-1,2,4-triazolo[1,5-*c*]pyrimidines (4**, **5**, **7**, **15**–**20**).** Amino compound **30** (0.5 g, 1.95 mmol) was dissolved in freshly distilled dioxane (15 mL) and the freshly prepared arylacyl azide (**21**–**29**) (5 eq) was added. The mixture was refluxed under argon for 18 h. Then the solvent was removed under reduced pressure and the residue was purified by flash chromatography (EtOAc-Methanol 9:1 gradient EtOAc-Methanol 8:2) on silica gel pretreated with ammonia gas, to afford the desired final compounds (**4**, **5**, **7**, **15**–**20**) as a solid 365 in a quite good yield.

5-[[[(3-Pyridyl)amino]carbonyl]amino-8-methyl-2-(2-furyl)pyrazolo[4,3-*e*]-1,2,4-triazolo[1,5-*c*]pyrimidine (5**):** yield 55%; pale yellow solid; mp 183 °C (methanol–diethyl ether); IR (KBr): 3245–2965, 1666, 1620, 1512, 1453 cm⁻¹; ¹H NMR (DMSO-*d*₆) δ: 4.09 (s, 3H); 6.74 (dd, 1H, *J* = 2, *J* = 4); 7.23 (d, 1H, *J* = 4); 7.36–7.41 (m, 1H); 7.91 (s, 1H); 7.94–8.01 (m, 1H); 8.37 (d, 1H, *J* = 2); 8.65–8.71 (m, 1H); 8.82 (s, 1H); 9.95 (bs, 1H); 10.60 (bs, 1H). ES-MS: (MH⁺) 376.5. Anal. (C₁₇H₁₃N₉O₂) C, H, N.

5-[[[(2-Pyridyl)amino]carbonyl]amino-8-methyl-2-(2-furyl)pyrazolo[4,3-*e*]-1,2,4-triazolo[1,5-*c*]pyrimidine (7**):** yield 64%; light brown solid; mp 175 °C (methanol–diethyl ether); IR (KBr): 3245–2968, 1665, 1615, 1510, 1450 cm⁻¹; ¹H NMR (DMSO-*d*₆) δ: 4.10 (s, 3H); 6.73 (dd, 1H, *J* = 2, *J* = 4); 7.02–7.19 (m, 1H); 7.22 (d, 1H, *J* = 4); 7.43–7.61 (m, 1H); 7.79–7.85 (m, 1H); 7.90–8.01 (m, 1H); 8.24 (d, 1H, *J* = 2); 8.72 (s, 1H); 8.95 (bs, 1H); 10.92 (bs, 1H). ES-MS: (MH⁺) 376.5. Anal. (C₁₇H₁₃N₉O₂) C, H, N.

5-[[[(3-Furyl)amino]carbonyl]amino-8-methyl-2-(2-furyl)pyrazolo[4,3-*e*]-1,2,4-triazolo[1,5-*c*]pyrimidine (15**):** yield 45%; brown solid; mp 182 °C (methanol–diethyl ether); IR (KBr): 3245–2970, 1660, 1610, 1510, 1445 cm⁻¹; ¹H NMR (DMSO-*d*₆) δ: 4.15 (s, 3H); 6.73–6.85 (m, 2H); 7.02–7.19 (m, 2H); 7.79–7.85 (m, 1H); 7.90–8.01 (m, 1H); 8.24 (d, 1H, *J* = 2); 8.74 (s, 1H); 8.97 (bs, 1H); 11.02 (bs, 1H). ES-MS: (MH⁺) 365.3. Anal. (C₁₆H₁₂N₈O₃) C, H, N.

5-[[[(3-Furyl)amino]carbonyl]amino-8-methyl-2-(2-furyl)pyrazolo[4,3-*e*]-1,2,4-triazolo[1,5-*c*]pyrimidine (16**):** yield 63%; brown solid; mp 193 °C (methanol–diethyl ether); IR (KBr): 3240–2985,

1665, 1610, 1520, 1450 cm^{-1} ; ^1H NMR (DMSO- d_6) δ : 4.08 (s, 3H); 6.62–6.73 (m, 2H); 7.22–7.35 (m, 2H); 7.59–7.65 (m, 1H); 7.95 (s, 1H); 8.11 (s, 1H); 8.63 (bs, 1H); 10.89 (bs, 1H). ES-MS: (MH^+) 365.3. Anal. ($\text{C}_{16}\text{H}_{12}\text{N}_8\text{O}_3$) C, H, N.

5-[[Benzofuran-2-yl]amino]carbonylamino-8-methyl-2-(2-furyl)-pyrazolo[4,3-*e*]-1,2,4-triazolo[1,5-*c*]pyrimidine (17): yield 58%; yellow solid; mp 192 °C (methanol–diethyl ether); IR (KBr): 3242–2975, 1668, 1610, 1515, 1460 cm^{-1} ; ^1H NMR (DMSO- d_6) δ : 4.09 (s, 3H); 6.79 (dd, 1H, $J = 2, J = 4$); 7.05–7.19 (m, 2H); 7.24 (d, 1H, $J = 4$); 7.42–7.59 (m, 2H); 8.01 (d, 1H, $J = 2$); 8.79 (s, 1H); 10.22 (bs, 1H); 11.59 (bs, 1H). ES-MS: (MH^+) 415.4. Anal. ($\text{C}_{20}\text{H}_{14}\text{N}_8\text{O}_3$) C, H, N.

5-[[Quinolin-2-yl]amino]carbonylamino-8-methyl-2-(2-furyl)-pyrazolo[4,3-*e*]-1,2,4-triazolo[1,5-*c*]pyrimidine (18): yield 60%; brown solid; mp 190 °C (methanol–diethyl ether); IR (KBr): 3240–2985, 1665, 1600, 1515, 1450 cm^{-1} ; ^1H NMR (DMSO- d_6) δ : 4.07 (s, 3H); 6.78 (dd, 1H, $J = 2, J = 4$); 7.22 (d, 1H, $J = 4$); 7.40–7.57 (m, 2H); 7.63–7.85 (m, 3H); 8.03 (d, 1H, $J = 2$); 8.23–8.31 (m, 1H); 8.67 (s, 1H); 10.21 (bs, 1H); 11.13 (bs, 1H). ES-MS: (MH^+) 426.4. Anal. ($\text{C}_{21}\text{H}_{15}\text{N}_9\text{O}_2$) C, H, N.

5-[[2-Methyl-thiophen-3-yl]amino]carbonylamino-8-methyl-2-(2-furyl)-pyrazolo[4,3-*e*]-1,2,4-triazolo[1,5-*c*]pyrimidine (19): yield 70%; brown solid; mp 195 °C (methanol–diethyl ether); IR (KBr): 3240–2975, 1670, 1605, 1510, 1455 cm^{-1} ; ^1H NMR (DMSO- d_6) δ : 2.27 (s, 3H); 4.05 (s, 3H); 6.34 (d, 1H, $J = 4$); 6.62 (dd, 1H, $J = 2, J = 4$); 6.98 (d, 1H, $J = 4$); 7.21 (d, 1H, $J = 4$); 7.78 (d, 1H, $J = 2$); 8.21 (s, 1H); 9.65 (bs, 1H); 11.38 (bs, 1H). ES-MS: (MH^+) 395.4. Anal. ($\text{C}_{17}\text{H}_{14}\text{N}_9\text{O}_2\text{S}$) C, H, N.

5-[[3-Methyl-thiophen-2-yl]amino]carbonylamino-8-methyl-2-(2-furyl)-pyrazolo[4,3-*e*]-1,2,4-triazolo[1,5-*c*]pyrimidine (20): yield 55%; brown solid; mp 170 °C (methanol–diethyl ether); IR (KBr): 3245–2965, 1667, 1615, 1513, 1445 cm^{-1} ; ^1H NMR (DMSO- d_6) δ : 2.39 (s, 3H); 4.05 (s, 3H); 6.62 (dd, 1H, $J = 2, J = 4$); 6.79 (d, 1H, $J = 4$); 6.97 (d, 1H, $J = 4$); 7.21 (d, 1H, $J = 4$); 7.82 (d, 1H, $J = 2$); 8.19 (s, 1H); 8.65 (bs, 1H); 10.01 (bs, 1H). ES-MS: (MH^+) 395.4. Anal. ($\text{C}_{17}\text{H}_{14}\text{N}_9\text{O}_2\text{S}$) C, H, N.

General Procedure for the Preparation of 5-[[Pyridyl]amino]carbonylamino-8-methyl-2-(2-furyl)-pyrazolo[4,3-*e*]-1,2,4-triazolo[1,5-*c*]pyrimidine Hydrochloride (3, 6, 8). Pyridyl derivative (**4**, **5**, **7**) (50 mg, 0.13 mmol) was dissolved in methanol (1 mL), and a saturated solution of methanol with HCl gas (2 mL) was added at 0 °C. The reaction was stirred at the same temperature for 30 min, and then the solvent was removed under reduced pressure to afford the correspondent salt as a solid in quantitative yield.

5-[[3-Pyridyl]amino]carbonylamino-8-methyl-2-(2-furyl)-pyrazolo[4,3-*e*]-1,2,4-triazolo[1,5-*c*]pyrimidine hydrochloride (6): white solid, mp 223–225 °C (dec) (methanol–diethyl ether); IR (KBr): 3425–2900, 1665, 1625, 1610, 1520, 1455 cm^{-1} ; ^1H NMR (D_2O) δ : 3.60 (s, 3H); 6.18 (dd, 1H, $J = 2, J = 4$); 6.57 (d, 1H, $J = 4$); 7.20 (d, 2H, $J = 9$); 7.61–7.78 (m, 1H); 7.80 (s, 1H); 7.95–8.01 (m, 1H); 8.21 (d, 1H, $J = 4$); 8.62 (s, 1H). Anal. ($\text{C}_{17}\text{H}_{14}\text{N}_9\text{O}_2\text{Cl}$) C, H, N.

5-[[2-Pyridyl]amino]carbonylamino-8-methyl-2-(2-furyl)-pyrazolo[4,3-*e*]-1,2,4-triazolo[1,5-*c*]pyrimidine hydrochloride (8): white solid, mp 223–225 °C (dec) (methanol–diethyl ether); IR (KBr): 3425–2900, 1665, 1625, 1610, 1520, 1455 cm^{-1} ; ^1H NMR (D_2O) δ : 3.62 (s, 3H); 6.21 (dd, 1H, $J = 2, J = 4$); 6.55 (d, 1H, $J = 4$); 7.18 (d, 2H, $J = 9$); 7.31–7.45 (m, 1H); 7.58 (s, 1H); 7.75–7.93 (m, 1H); 8.23 (s, 1H). Anal. ($\text{C}_{17}\text{H}_{14}\text{N}_9\text{O}_2\text{Cl}$) C, H, N.

General Procedures for the Preparation of [3-(2-Furan-2-yl-8-methy-8H-pyrazolo[4,3-*e*][1,2,4]triazolo[1,5-*c*]pyrimidin-5-yl)-ureido]-*N*-methylpyridinium Iodide Derivatives (9–11). Pyrido derivative (**4**, **5**, **7**) (50 mg, 0.13 mmol) was dissolved in acetonitrile (10 mL), and a slight excess of methyl iodide (2 equivalents) was added. The reaction was stirred at 40 °C for 5 h. Then the solvent was removed under reduced pressure to afford the corresponding salt as a solid in quantitative yield.

4-[3-(2-Furan-2-yl-8-methy-8H-pyrazolo[4,3-*e*][1,2,4]triazolo[1,5-*c*]pyrimidin-5-yl)-ureido]-*N*-methylpyridinium iodide (9): yellow solid; mp 221 °C (dec) (methanol–diethyl ether); IR

(KBr): 3340–2750, 1665, 1615, 1610, 1505, 1450 cm^{-1} ; ^1H NMR (DMSO- d_6) δ : 3.41 (s, 3H); 4.07 (s, 3H); 6.78 (dd, 1H, $J = 2, J = 4$); 7.21 (d, 1H, $J = 4$); 7.99 (d, 2H, $J = 9$); 8.01 (d, 1H, $J = 2$); 8.65 (d, 2H, $J = 9$); 8.79 (s, 1H); 9.05 (bs, 1H); 11.18 (bs, 1H). ES-MS: (MH^+) 391.4. Anal. ($\text{C}_{18}\text{H}_{16}\text{N}_9\text{O}_2\text{I}$) C, H, N.

3-[3-(2-Furan-2-yl-8-methy-8H-pyrazolo[4,3-*e*][1,2,4]triazolo[1,5-*c*]pyrimidin-5-yl)-ureido]-*N*-methylpyridinium iodide (10): yellow solid; mp 224 °C (methanol–diethyl ether); IR (KBr): 3335–2760, 1668, 1615, 1605, 1515, 1465 cm^{-1} ; ^1H NMR (DMSO- d_6) δ : 3.43 (s, 3H); 4.05 (s, 3H); 6.68 (dd, 1H, $J = 2, J = 4$); 7.21 (d, 1H, $J = 4$); 7.35–7.42 (m, 1H); 7.95 (s, 1H); 7.97–8.03 (m, 1H); 8.21 (d, 1H, $J = 4$); 8.61–8.75 (m, 1H); 8.79 (s, 1H). 9.99 (bs, 1H); 10.61 (bs, 1H). ES-MS: (MH^+) 391.4. Anal. ($\text{C}_{18}\text{H}_{16}\text{N}_9\text{O}_2\text{I}$) C, H, N.

2-[3-(2-Furan-2-yl-8-methy-8H-pyrazolo[4,3-*e*][1,2,4]triazolo[1,5-*c*]pyrimidin-5-yl)-ureido]-*N*-methylpyridinium iodide (11): yellow solid; mp 194 °C (methanol–diethyl ether); IR (KBr): 3350–2770, 1670, 1625, 1610, 1510, 1455 cm^{-1} ; ^1H NMR (DMSO- d_6) δ : 3.18 (s, 1H); 4.06 (s, 3H); 6.79 (dd, 1H, $J = 2, J = 4$); 7.05–7.19 (m, 1H); 7.25 (d, 1H, $J = 4$); 7.59–7.91 (m, 2H); 8.04 (d, 1H, $J = 2$); 8.21–8.25 (d, 1H, $J = 2$); 8.79 (s, 1H); 8.90 (bs, 1H); 10.87 (bs, 1H). ES-MS: (MH^+) 391.4. Anal. ($\text{C}_{18}\text{H}_{16}\text{N}_9\text{O}_2\text{I}$) C, H, N.

General Procedures for the Preparation of [3-(2-Furan-2-yl-8-methy-8H-pyrazolo[4,3-*e*][1,2,4]triazolo[1,5-*c*]pyrimidin-5-yl)-ureido]-pyridinium *N*-Oxide Derivatives (12–14). Pyrido derivative (**4**, **5**, **7**) (50 mg, 0.13 mmol) was dissolved in dry THF (10 mL), and an excess of mCPBA (3 equivalents) was added. The reaction was stirred at room temperature for 12 h. The final products precipitated from reaction mixture that was filtered off as a solid in high yield.

4-[3-(2-Furan-2-yl-8-methy-8H-pyrazolo[4,3-*e*][1,2,4]triazolo[1,5-*c*]pyrimidin-5-yl)-ureido]pyridinium *N*-oxide (12): yield 75%; pale yellow solid; mp 198 °C (methanol–diethyl ether); IR (KBr): 3345–2745, 1668, 1615, 1610, 1505, 1450 cm^{-1} ; ^1H NMR (DMSO- d_6) δ : 4.05 (s, 3H); 6.77 (dd, 1H, $J = 2, J = 4$); 7.20 (d, 1H, $J = 4$); 7.59 (d, 2H, $J = 9$); 7.99 (d, 1H, $J = 2$); 8.21 (d, 2H, $J = 9$); 8.65 (s, 1H); 9.15 (bs, 1H); 10.98 (bs, 1H). ES-MS: (MH^+) 392.3. Anal. ($\text{C}_{17}\text{H}_{13}\text{N}_9\text{O}_3$) C, H, N.

3-[3-(2-Furan-2-yl-8-methy-8H-pyrazolo[4,3-*e*][1,2,4]triazolo[1,5-*c*]pyrimidin-5-yl)-ureido]pyridinium *N*-oxide (13): yield 80%; pale yellow solid; mp 185 °C (methanol–diethyl ether); IR (KBr): 3245–2975, 1665, 1620, 1520, 1450 cm^{-1} ; ^1H NMR (DMSO- d_6) δ : 4.04 (s, 3H); 6.78 (dd, 1H, $J = 2, J = 4$); 7.21 (d, 1H, $J = 4$); 7.38–7.44 (m, 1H); 7.96 (s, 1H); 7.99–8.07 (m, 1H); 8.47 (d, 1H, $J = 2$); 8.75–8.91 (m, 1H); 8.95 (s, 1H); 9.65 (bs, 1H); 10.73 (bs, 1H). ES-MS: (MH^+) 392.3. Anal. ($\text{C}_{17}\text{H}_{13}\text{N}_9\text{O}_3$) C, H, N.

2-[3-(2-Furan-2-yl-8-methy-8H-pyrazolo[4,3-*e*][1,2,4]triazolo[1,5-*c*]pyrimidin-5-yl)-ureido]pyridinium *N*-oxide (14): yield 78%; pale yellow solid; mp 192 °C (methanol–diethyl ether); IR (KBr): 3255–2975, 1668, 1610, 1511, 1465 cm^{-1} ; ^1H NMR (DMSO- d_6) δ : 4.06 (s, 3H); 6.68 (dd, 1H, $J = 2, J = 4$); 7.00–7.15 (m, 1H); 7.20 (d, 1H, $J = 4$); 7.36–7.41 (m, 1H); 7.75–7.82 (m, 1H); 7.97–8.04 (m, 1H); 8.27 (d, 1H, $J = 2$); 8.79 (s, 1H); 10.95 (bs, 1H); 12.01 (bs, 1H). ES-MS: (MH^+) 392.3. Anal. ($\text{C}_{17}\text{H}_{13}\text{N}_9\text{O}_3$) C, H, N.

Biology. CHO Membrane Preparation. The expression of the human A_1 , $\text{A}_{2\text{A}}$, and A_3 receptors in CHO cells has been previously described.³⁵ The cells were grown adherently and maintained in Dulbecco's modified Eagle's medium with nutrient mixture F12 without nucleosides at 37 °C in 5% $\text{CO}_2/95\%$ air. Cells were split two or three times weekly, and then the culture medium was removed for membrane preparations. The cells were washed with phosphate-buffered saline solution and scraped off flasks in ice-cold hypotonic buffer (5 mM Tris HCl, 2 mM EDTA, pH 7.4). The cell suspension was homogenized with a Polytron, and the homogenate was centrifuged for 30 min at 48 000g. The membrane pellet was resuspended in 50 mM Tris HCl buffer at pH 7.4 for A_1 adenosine receptors, in 50 mM Tris HCl, 10 mM MgCl_2 at pH 7.4 for $\text{A}_{2\text{A}}$ adenosine receptors, in 50 mM Tris HCl, 10 mM MgCl_2 ,

1 mM EDTA at pH 7.4 for A₃ adenosine receptors, and were utilized for the binding assay.

Human Cloned A₁, A_{2A}, and A₃ Adenosine Receptor Binding Assay. Binding of [³H]-DPCPX to CHO cells transfected with the human recombinant A₁ adenosine receptor was performed as previously described.²⁸ Displacement experiments were performed for 120 min at 25 °C in 0.20 mL of buffer containing 1 nM [³H]-DPCPX, 20 mL of diluted membranes (50 mg of protein/assay) and at least 6–8 different concentrations of examined compounds. Nonspecific binding was determined in the presence of 10 mM of CHA, and this is always ≤10% of the total binding. Binding of [³H]-ZM241385 to CHO cells transfected with the human recombinant A_{2A} adenosine receptors (50 mg of protein/assay) was performed according to Ongini et al.³⁰ In competition studies, at least 6–8 different concentrations of compounds were used and nonspecific binding was determined in the presence of 50 mM NECA for an incubation time of 60 min at 25 °C.

Binding of [³H]MRE3008-F20 to CHO cells transfected with the human recombinant A₃ adenosine receptors was performed according to Varani et al.²⁹ Competition experiments were carried out in duplicate in a final volume of 250 mL in test tubes containing 1 nM [³H] MRE3008-F20, 50 mM Tris HCl buffer, 10 mM MgCl₂, pH 7.4, and 100 mL of diluted membranes (50 mg protein/assay), and at least 6–8 different concentrations of examined ligands. Incubation time was 120 min at 4 °C, according to the results of previous time-course experiments.²⁹ Nonspecific binding was defined as binding in the presence of 1 mM of MRE3008-F20 and was about 25% of total binding. Bound and free radioactivities were separated by filtering the assay mixture through Whatman GF/B glass-fiber filters using a Micro-Mate 196 cell harvester (Packard Instrument Company). The filter bound radioactivity was counted on Top Count (efficiency 57%) with Micro-Scint 20. The protein concentration was determined according to the Bio-Rad method³⁶ with bovine albumin as reference standard.

Measurement of Cyclic AMP Levels in CHO Cells Transfected with Human A_{2B} Adenosine Receptors. CHO cells transfected with human A_{2B} adenosine receptors were washed with phosphate-buffered saline and diluted trypsin and centrifuged for 10 min at 200g. The pellet containing the CHO cells (1 × 10⁶ cells/assay) was suspended in 0.5 mL of incubation mixture (mM): NaCl 15, KCl 0.27, NaH₂PO₄ 0.037, MgSO₄ 0.1, CaCl₂ 0.1, HEPES 0.01, MgCl₂ 1, glucose 0.5, pH 7.4 at 37 °C, 2 IU/mL adenosine deaminase, and 4-(3-butoxy-4-methoxybenzyl)-2-imidazolidinone (Ro 20-1724) as phosphodiesterase inhibitor and preincubated for 10 min in a shaking bath at 37 °C. The potency of studied antagonists was determined by antagonism of NECA (100 nM)-induced stimulation of cyclic AMP levels. The reaction was terminated by the addition of cold 6% trichloroacetic acid (TCA). The TCA suspension was centrifuged at 2000g for 10 min at 4 °C, and the supernatant was extracted four times with water-saturated diethyl ether. The final aqueous solution was tested for cyclic AMP levels by a competition protein binding assay. Samples of cyclic AMP standard (0–10 pmol) were added to each test tube containing the incubation buffer (trizma base 0.1 M, aminophylline 8.0 mM, 2 mercaptoethanol 6.0 mM, pH 7.4) and [³H] cyclic AMP in a total volume of 0.5 mL. The binding protein previously prepared from beef adrenals was added to the samples previously incubated at 4 °C for 150 min and, after the addition of charcoal, were centrifuged at 2000g for 10 min. The clear supernatant was counted in a Beckman scintillation counter.

Computational Methodologies. All molecular modeling studies were carried out on a 10 CPU (AMD 64Athon and PIV 2.0–30 GHz) Linux cluster running under openMosix architecture.³⁷ Homology modeling, energy calculation, and docking studies have been done using Molecular Operating Environment (MOE, version 2004.03) suite.³⁸ Quantum calculations used throughout this study were performed using MOPAC (version 7.0).³⁹

Homology Model of the Resting State of Human A₃ Receptor. On the basis of the assumption that GPCRs share similar TM boundaries and overall topology, a homology model of the human A₃ receptor was constructed. First, the amino acid sequences of

TM helices of the resting state A₃ receptor were aligned with those of bovine rhodopsin, guided by the highly conserved amino acid residues, including the DRY motif (D3.49, R3.50, and Y3.51) and three Pro residues (P4.60, P6.50, and P7.50) in the TM segments of GPCRs. The same boundaries were applied for the TM helices of the A₃ receptor as were identified from the X-ray crystal structure for the corresponding sequences of bovine rhodopsin,⁴⁰ the C_R coordinates which were used to construct the seven TM helices for the human A₃ receptor. The loop domains of the human A₃ receptor were constructed by the loop search method implemented in MOE. In particular, loops are modeled first, in random order. For each loop, a contact energy function analyzes the list of candidates collected in the segment searching stage, taking into account all atoms already modeled and any atom specified by the user as belonging to the model environment. These energies are then used to make a Boltzmann-weighted choice from the candidates, the coordinates of which are then copied to the model. Any missing side chain atoms are modeled using the same procedure. Side chains belonging to residues, whose backbone coordinates were copied from a template, are modeled first, followed by side chains of modeled loops. Outgaps and their side chains are modeled last. Special caution had to be given to the second extracellular (E2) loop, which has been described in bovine rhodopsin to fold back over transmembrane helices,⁴⁰ and, therefore, it limits the size of the active site. Hence, amino acids of this loop could be involved in direct interactions with the ligands. The presence of a disulfide bridge between cysteines in TM3 and E2 might be the driving force to this peculiar fold of the E2 loop. Since this covalent link is conserved in all receptors modeled in the current study, the E2 loop was modeled using a rhodopsin-like constrained geometry around the E2-TM3 disulfide bridge. After the heavy atoms were modeled, all hydrogen atoms were added, and the protein coordinates were minimized with MOE using the AMBER94 force field.⁴¹ The minimizations were carried out by 1000 steps of steepest descent followed by conjugate gradient minimization until the rms gradient of the potential energy was less than 0.1 kcal mol⁻¹ Å⁻¹.

Molecular Docking of the Human A₃ Receptor Antagonists. All antagonist structures were docked into the hypothetical TM binding site by using the MULTIDOCK docking program, which is part of the MOE suite. Conformational samplings were conducted within a user-specified 3D docking box, using the Tabù Search protocol⁴² and MMFF94 force field.⁴⁴ MOE-Dock performs a user-specified number of independent docking runs (50 in our specific case) and wrote the resulting conformations and their energies in a molecular database file. The resulting docked complexes were subjected to MMFF94 energy minimization until the rms of the conjugate gradient was <0.1 kcal mol⁻¹ × Å⁻¹. Charges for the ligands were imported directly from the MMFF94 force field.

The interaction energy values were calculated as follows: $\Delta E_{\text{binding}} = E_{\text{complex}} - (E_{\text{ligand}} + E_{\text{receptor}})$. These energies are not rigorous thermodynamic quantities, but can only be used to compare the relative stabilities of the complexes. Therefore, these interaction energy values cannot be used to calculate binding affinities since changes in entropy and solvation effects are not taken into account.

Acknowledgment. We thank the Regione Friuli Venezia Giulia (Fondo 2000) for financial support. The molecular modeling work coordinated by S. Moro has been carried out with financial support of the University of Padova, Italy, and the Italian Ministry for University and Research (MIUR), Rome, Italy. S. Moro is also very grateful to Chemical Computing Group for the scientific and technical partnership.

Supporting Information Available: Elemental analysis table; figure showing the best docked conformation of the thiophene derivative. This material is available free of charge via the Internet at <http://pubs.acs.org>

References

- 1) Fredholm, B. B.; Ijzerman, A. P.; Jacobson, K. A.; Klotz, K. N.; Linden, J. *International Union of Pharmacology. XXV. Nomenclature and classification of adenosine receptors. Pharmacol. Rev.* **2001**, *53*, 527–552.

- (2) Jacobson, K. A.; Knutsen, L. J. S. P1 and P2 purine and pyrimidine receptor ligands. In *Handbook of Experimental Pharmacology*; Springer: Berlin, 2001, Vol. 151/1 (purinergic and pyrimidnergic Signalling I), pp 129–175.
- (3) Jacobson, K. A.; Suzuki, F. Recent developments in selective agonists and antagonists acting at purine and pyrimidine receptors. *Drug. Dev. Res.* **1996**, *39*, 289–300.
- (4) Meyerhof, W.; Muller-Brechlin, R.; Richter, D. Molecular cloning of a novel putative G-protein coupled receptor expressed during rat spermiogenesis. *FEBS Lett.* **1991**, *284*, 155–160.
- (5) Sajjadi, F. G.; Firestein, G. S. cDNA cloning and sequence analysis of the human A₃ adenosine receptor. *Biochim. Biophys. Acta* **1993**, *1179*, 105–107.
- (6) Salvatore, C. A.; Jacobson, M. A.; Taylor, H. E.; Linden, J.; Johnson, R. G. Molecular cloning and characterization of the human A₃ adenosine receptor. *Proc. Natl. Acad. Sci. U.S.A.* **1993**, *90*, 10365–10369.
- (7) Linden, J. Cloned adenosine A₃ receptors: Pharmacological properties, species differences and receptor functions. *Trends Pharmacol. Sci.* **1994**, *15*, 298–306.
- (8) Zhao, Z. H.; Ravid, S.; Ravid, K. Chromosomal mapping of the mouse A₃ adenosine receptor gene, adora3. *Genomics* **1995**, *30*, 118–119.
- (9) Hill, R. J.; Oleynek, J. J.; Hoth, C. F.; Kiron, M. A.; Weng, W. F.; Wester, R. T.; Tracey, W. R.; Knight, D. R.; Buchholz, R.; Kennedy, S. P. Cloning, expression and pharmacological characterization of rabbit A₁ and A₃ receptors. *J. Pharmacol. Exp. Ther.* **1997**, *280*, 122–128.
- (10) Abbracchio, M. P.; Brambilla, R.; Kim, H. O.; von Lubitz, D. K. J. E.; Jacobson, K. A.; Cattabeni, F. G-protein-dependent activation of phospholipase-C by adenosine A₃ receptor in rat brain. *Mol. Pharmacol.* **1995**, *48*, 1038–1045.
- (11) Ali, H.; Choi, O. H.; Fraundorfer, P. F.; Yamada, K.; Gonzaga, H. M. S.; Beaven, M. A. Sustained activation of phospholipase-D via adenosine A₃ receptors is associated with enhancement of antigenophore-induced and Ca²⁺-ionophore-induced secretion in a rat mast-cell line. *J. Pharmacol. Exp. Ther.* **1996**, *276*, 837–845.
- (12) Rorke, S.; Holgate, S. T. Targeting adenosine receptors: novel therapeutic targets in asthma and chronic obstructive pulmonary disease. *Am. J. Respir. Med.* **2002**, *1*, 99–105.
- (13) Merighi, S.; Mirandola, P.; Varani, K.; Gessi, S.; Leung, E.; Baraldi, P. G.; Tabrizi, M. A.; Borea, P. A. A glance at adenosine receptors: novel target for antitumor therapy. *Pharmacol. Ther.* **2003**, *100*, 31–48.
- (14) Brambilla, R.; Cattabeni, F.; Ceruti, S.; Barbieri, D.; Franceschi, C.; Kim, Y.; Jacobson, K. A.; Klotz, K. N.; Lohse, M. J.; Abbracchio, M. P. Activation of the A₃ adenosine receptor effects cell cycle progression and cell growth. *Naunyn-Schmiedeberg's Arch. Pharmacol.* **2000**, *361*, 225–234.
- (15) Baraldi, P. G.; Cacciari, B.; Romagnoli, R.; Merighi, S.; Varani, K.; Borea, P. A.; Spalluto, G. A₃ Adenosine receptor ligands; history and perspectives. *Med. Res. Rev.* **2000**, *20*, 103–128.
- (16) Moro, S.; Deflorian, F.; Spalluto, G.; Pastorin, G.; Cacciari, B. et al. Demystifying the three-dimensional structure of G protein-coupled receptors (GPCRs) with the aid of molecular modeling. *Chem. Commun. (Camb)* **2003**, 2949–2956.
- (17) Jacobson, K. A.; Tchilibon, S.; Joshi, B. V.; Gao, Z. G. A₃ adenosine receptors. In *Annual Reports in Medicinal Chemistry*, 1st ed.; Doherty, A. M., Ed.; Elsevier: New York, 2003; pp 121–130.
- (18) Baraldi, P. G.; Cacciari, B.; Romagnoli, R.; Spalluto, G.; Klotz, K. N.; Leung, E.; Varani, K.; Gessi, S.; Merighi, S.; Borea, P. A. Pyrazolo[4,3-*e*]1,2,4-triazolo[1,5-*c*]pyrimidine derivatives as highly potent and selective human A₃ adenosine receptor antagonists. *J. Med. Chem.* **1999**, *42*, 4473–4478.
- (19) Baraldi, P. G.; Cacciari, B.; Romagnoli, R.; Spalluto, G.; Moro, S.; Klotz, K. N.; Leung, E.; Varani, K.; Gessi, S.; Merighi, S.; Borea, P. A. Pyrazolo[4,3-*e*]1,2,4-triazolo[1,5-*c*]pyrimidine derivatives as highly potent and selective human A₃ adenosine receptor antagonists: Influence of the chain at N⁸ pyrazole nitrogen. *J. Med. Chem.* **2000**, *43*, 4768–4780.
- (20) Baraldi, P. G.; Cacciari, B.; Moro, S.; Spalluto, G.; Pastorin, G.; Da Ros, T.; Klotz, K. N.; Varani, K.; Gessi, S.; Borea, P. A. Synthesis, Biological Activity, and Molecular Modeling Investigation of New Pyrazolo[4,3-*e*]1,2,4-triazolo[1,5-*c*]pyrimidine Derivatives as Human A₃ Adenosine Receptor Antagonists. *J. Med. Chem.* **2002**, *45*, 770–780.
- (21) Pastorin, G.; Da Ros, T.; Spalluto, G.; Deflorian, F.; Moro, S.; Cacciari, B.; Baraldi, P. G.; Gessi, S.; Varani, K.; Borea, P. A. Pyrazolo[4,3-*e*]1,2,4-triazolo[1,5-*c*]pyrimidine derivatives as adenosine receptor antagonists. Influence of the N5 substituent on the affinity at the human A₃ and A_{2B} adenosine receptor subtypes: a molecular modeling investigation. *J. Med. Chem.* **2003**, *46*, 4287–96.
- (22) Maconi, A.; Pastorin, G.; Da Ros, T.; Spalluto, G.; Gao, Z. G.; Jacobson, K. A.; Baraldi, P. G.; Cacciari, B.; Varani, K.; Borea, P. A. Synthesis, biological properties and molecular modeling investigation of the first potent, selective and water soluble human A₃ adenosine receptor antagonist. *J. Med. Chem.* **2002**, *45*, 3579–3582.
- (23) Saikachi, H.; Kitagawa, T.; Nasu, A.; Sasaki, H. Synthesis of Furan Derivatives LXXXVII. *Chem. Pharm. Bull.* **1981**, *29*, 237–244.
- (24) Curtius, T.; Mohr, E. Ueberführung von nicotinsäure in β amidopyridin. *Ber.* **1898**, *31*, 2493–2495.
- (25) Gatta, F.; Del Giudice, M. R.; Borioni, A.; Borea, P. A.; Dionisotti, S.; Ongini, E. Synthesis of imidazo[1,2-*c*]pyrazolo[4,3-*e*] pyrimidines, pyrazolo[4,3-*e*]1,2,4-triazolo[1,5-*c*]pyrimidines and triazolo[5,1-*i*]purines: new potent A₂ adenosine receptor antagonists. *Eur. J. Med. Chem.* **1993**, *28*, 569–577.
- (26) Schmidt, P.; Eichenberger, K.; Wilhelm, M.; Druey, J. Pyrazolopyrimidine III. *Helv. Chim. Acta* **1959**, *39*, 349–359.
- (27) Todd, D. The Wolff–Kishner reduction. *J. Am. Chem. Soc.* **1949**, *71*, 1353–1355.
- (28) Lohse, M. J.; Klotz, K. N.; Lindernborn-Fotinos, J.; Reddington, M.; Schwabe, U.; Olsson, R. A. 8-Cyclopentyl 1,3-dipropylxanthine DPCPX a selective high affinity antagonist radioligand for A₁ adenosine receptors. *Naunyn-Schmiedeberg's Arch. Pharmacol.* **1987**, *336*, 204–210.
- (29) Varani, K.; Merighi, S.; Gessi, S.; Klotz, K. N.; Leung, E.; Baraldi, P. G.; Cacciari, B.; Spalluto, G.; Borea, P. A. [³H]MRE3008-F20: a novel antagonist radioligand for the pharmacological and biochemical characterization of human A₃ adenosine receptors. *Mol. Pharmacol.* **2000**, *57*, 968–975.
- (30) Ongini, E.; Dionisotti, S.; Gessi, S.; Irenius, E.; Fredholm, B. B. Comparison of CGS 15943 and SCH 58261 as antagonist at human A₃ adenosine receptors. *Naunyn Schmiedeberg's Arch. Pharmacol.* **1999**, *359*, 7–10.
- (31) Hansch, C.; Leo, A.; Taft, R. W. A survey of Hammett substituent. Constants and resonance and field parameters. *Chem. Rev.* **1991**, *91*, 165–195.
- (32) Moro, S.; Spalluto, G.; Jacobson, K. A. Techniques: Recent developments in computer-aided engineering of GPCR ligands using the human A₃ adenosine receptor as an example. *Trends Pharmacol. Sci.* **2005**, *26*, 44–51.
- (33) Moro, S.; Braiuca, P.; Deflorian, F.; Ferrari, C.; Pastorin, G.; Cacciari, B.; Baraldi, P. G.; Varani, K.; Borea, P. A.; Spalluto, G. Combined Target-based and Ligand-based Drug Design Approach as Tool to Define a Novel 3D-Pharmacophore Model of Human A₃ Adenosine Receptor Antagonists: Pyrazolo[4,3-*e*]1,2,4-Triazolo[1,5-*c*]Pyrimidine Derivatives as a Key Study. *J. Med. Chem.* **2005**, *48*, 152–162.
- (34) Gao, Z. G.; Chen, A.; Barak, D.; Kim, S. K.; Muller, C. E. et al. Identification by site-directed mutagenesis of residues involved in ligand recognition and activation of the human A₃ adenosine receptor. *J. Biol. Chem.* **2002**, *277*, 19056–19063.
- (35) Klotz, K. N.; Hessling, J.; Hegler, J.; Owman, C.; Kull, B.; Fredholm, B. B.; Lohse, M. J. Comparative pharmacology of human adenosine receptor subtypes- characterization of stably transfected receptors in CHO cells. *Naunyn-Schmiedeberg's Arch. Pharmacol.* **1998**, *357*, 1–9.
- (36) Bradford, M. M. A rapid sensitive method for the quantification of microgram quantities of protein utilizing the principle of protein dye-binding. *Anal. Biochem.* **1976**, *72*, 248–254.
- (37) OpenMosix: <http://www.openMosix.org>, 2004.
- (38) Molecular Operating Environment (MOE 2004.03), C. C. G., Inc, 1255 University St., Suite 1600, Montreal, Quebec, Canada, H3B 3 × 3.
- (39) MOPAC available from Quantum Chemistry Program Exchange., ver.6.0.
- (40) Palczewski, K.; Kumasaka, T.; Hori, T.; Behnke, C. A.; Motoshima, H. et al. Crystal structure of rhodopsin: A G protein-coupled receptor. *Science* **2000**, *289*, 739–745.
- (41) Cornell, W. D. C., P.; Bayly, C. I.; Gould, I. R.; Merz, K. M.; Ferguson, D. M.; Spellmeyer, D. C.; Fox, T.; Caldwell, J. W.; Kollman, P. A. A second generation force field for the simulation of proteins, nucleic acids and organic molecules. *J. Am. Chem. Soc.* **1995**, *117*, 5179–5196.
- (42) Baxter, C. A.; Murray, C. W.; Clark, D. E.; Westhead, D. R.; Eldridge, M. D. Flexible Docking Using Tabu Search and an Empirical Estimate of Binding Affinity. *Proteins: Struct., Funct. Genet.* **1998**, *33*, 367–382.
- (43) Halgren, T. Merck Molecular Force Field. I. Basis, Form, Scope, Parameterization, and Performance of MMFF94. *J. Comput. Chem.* **1996**, *17*, 490–519.